ENVIRONMENTAL RESEARCH
LETTERS

CrossMark

OPEN ACCESS

RECEIVED
25 April 2024

REVISED
7 June 2024

ACCEPTED FOR PUBLICATION
4 July 2024

PUBLISHED
12 July 2024

LETTER

Elevated CO_2 concentrations contribute to a closer relationship between vegetation growth and water availability in the Northern Hemisphere mid-latitudes

Yang Song[1,2], **Yahui Guo**[3,4], **Shijie Li**[5], **Wangyipu Li**[6,7] **and Xiuliang Jin**[1,2,*]

[1] Institute of Crop Sciences, Chinese Academy of Agricultural Sciences/State Key Laboratory of Crop Physiology and Ecology, Ministry of Agriculture and Rural Affairs of China, Beijing, People's Republic of China
[2] National Nanfan Research Institute (Sanya), Chinese Academy of Agricultural Sciences, Sanya, People's Republic of China
[3] College of Urban and Environmental Sciences, Central China Normal University, Wuhan, People's Republic of China
[4] Key Laboratory of Green Pesticide, Central China Normal University, Wuhan, People's Republic of China
[5] School of Geographical Sciences, Nanjing University of Information Science and Technology, Nanjing, People's Republic of China
[6] Institute of Remote Sensing and Geographic Information System, School of Earth and Space Sciences, Peking University, Beijing, People's Republic of China
[7] Beijing Key Laboratory of Spatial Information Integration and Its Applications, Beijing, People's Republic of China
[*] Author to whom any correspondence should be addressed.

E-mail: jinxiuliang@caas.cn, songyang.rs@hotmail.com, guoyh@ccnu.edu.cn, lishijie@nuist.edu.cn and lwyp_sess@stu.pku.edu.cn

Keywords: climate change, terrestrial ecosystems, remote sensing, NDVI, PDSI, carbon dioxide

Abstract

The Northern Hemisphere mid-latitudes, with large human populations and terrestrial carbon sinks, have a high demand for and dependence on water resources. Despite the growing interest in vegetation responses to drought under climate change in this region, our understanding of changes in the relationship between vegetation growth and water availability (referred to as Rvw) remains limited. Here, we aim to explore the Rvw and its drivers in the Northern Hemisphere mid-latitudes between 1982 and 2015. We used the satellite-derived normalized difference vegetation index (NDVI) and the fine-resolution Palmer drought severity index (PDSI) as proxies for vegetation growth and water availability, respectively. The trend analysis results showed that changes in NDVI and PDSI were asynchronous over the past three decades. Moreover, we analyzed the spatiotemporal patterns of the correlation coefficient between NDVI and PDSI. The results indicated that the Rvw was getting closer in more areas over the period, but there were differences across ecosystems. Specifically, most croplands and grasslands were primarily constrained by water deficit, which was getting stronger; however, most forests were primarily constrained by water surplus, which was getting weaker. Furthermore, our random forest regression models indicated that the dominant driver of changes in the NDVI-PDSI correlation was atmospheric carbon dioxide (CO_2) in more than 45% of grid cells. In addition, the partial correlation analysis results demonstrated that elevated CO_2 concentrations not only boosted vegetation growth through the fertilizer effect but also indirectly enhanced water availability by improving water use efficiency. Overall, this study highlights the important role of atmospheric CO_2 in mediating the Rvw under climate change, implying a potential link between vegetation greening and drought risk.

1. Introduction

The relationship between vegetation growth and water availability (referred to as Rvw), representing vegetation responses to water availability, is a key metric for understanding vegetation responses to drought under climate change (Shi *et al* 2021, Zhao *et al* 2021b, Chen *et al* 2022, Smith and Boers 2023). Over the past few decades, global vegetation growth has been observed to increase, a phenomenon known as 'greening' (Myneni *et al* 1997, Zhu *et al* 2016, Huang *et al* 2018, Piao *et al* 2020). The vegetation greening trend, attributed to factors such as the carbon dioxide (CO_2) fertilization effect, climate warming, and human activities, has been widely studied (Piao *et al* 2015, 2020, Lu *et al* 2016, Zhu *et al* 2016). However, changes in vegetation growth are also associated with water availability, representing a potential threat to the recent greening trend (Jiao *et al* 2021, Chen *et al* 2022, Wei *et al* 2023). For cropland, grassland, and forest ecosystems, too much or too little water can undermine normal vegetation growth. At the same time, the sharp boost in vegetation productivity will also enhance vegetation water demand in these ecosystems to some extent (Chen *et al* 2022, Denissen *et al* 2022, Abel *et al* 2023). Therefore, it is essential to understand changes in the Rvw to effectively evaluate current and future drought risk.

The Northern Hemisphere mid-latitudes are a hotspot for study. Previous studies have expressed a strong interest in its vegetation response to drought (Wu *et al* 2017, Peng *et al* 2019, Jiao *et al* 2021, Zhao *et al* 2021a). Multiple lines of observed evidence suggest that water deficit areas were significantly expanding while water surplus areas were significantly shrinking (Jiao *et al* 2021). Climate factors and atmospheric CO_2 are considered to have significant impacts on both vegetation growth and water availability. Climate warming can increase vegetation productivity by lengthening the active growth season and improving the maximum photosynthetic rate, but it can also result in greater water loss (Myneni *et al* 1997, Nemani *et al* 2003, Bastos *et al* 2019). Rising vapor pressure deficit (VPD) can reduce stomatal conductance and limit the actual photosynthetic rate, but can also decrease plant transpiration and thereby mitigate drought stress (Jung *et al* 2010, Novick *et al* 2016, Yuan *et al* 2019). The CO_2 fertilization effect has benefits for both vegetation growth and water use efficiency (WUE) (Lu *et al* 2016, Humphrey *et al* 2018, Wang *et al* 2020, Hsu and Dirmeyer 2023). Although human activities such as land use/land cover change and cropping intensity also influence both (Chen *et al* 2019b), their role remains limited compared to climate change at a global scale (Bastos *et al* 2019). However, the dominant driver of changes in the Rvw needs to contribute to both at the same time, that is, it should not only enhance (or reduce) vegetation growth but also be able to increase (or decrease) water availability. Therefore, it remains a challenge to determine which one factor plays a dominant role.

Here, we aim to investigate the Rvw and its drivers in the Northern Hemisphere mid-latitudes during 1982–2015. We used the normalized difference vegetation index (NDVI) as a proxy for vegetation growth and the Palmer drought severity index (PDSI) as a proxy for water availability (Pinzon and Tucker 2014, Abatzoglou *et al* 2018). We explored the long-term trends in NDVI and PDSI to determine whether there was a strong coupling between them. The Spearman's rank correlation between NDVI and PDSI (hereafter referred to as the NDVI-PDSI correlation) was used to characterize the Rvw for each grid cell (Jiao *et al* 2021). We evaluated the NDVI-PDSI correlation for the entire study period and then used 25 10 year moving windows spanning from 1982 to 2015 to estimate the trend in the NDVI-PDSI correlation coefficient (Schwalm *et al* 2017, Vicente-Serrano *et al* 2013, Doughty *et al* 2015, Peters *et al* 2018, Jiao *et al* 2021). Moreover, we examined the different spatiotemporal patterns of the NDVI-PDSI correlation for croplands, grasslands, and forests. Finally, we employed random forest regression models to reveal the dominant driver of changes in the NDVI-PDSI correlation for each grid cell by ranking the feature importance (Yuan *et al* 2019, Chang *et al* 2023, Dong *et al* 2023, Yang *et al* 2024). To further reveal how the dominant driver affected changes in the Rvw, we conducted the partial correlation analysis to evaluate its roles on NDVI and PDSI individually (Yuan *et al* 2019, Song *et al* 2022). By introducing WUE, we explored the indirect effect of the dominant driver on water availability (Tian *et al* 2021). In this study, our findings are expected to advance an in-depth understanding of changes in the Rvw under climate change, thereby highlighting a potential link between vegetation greening and drought risk.

2. Materials and methods

2.1. Data

The third-generation Global Inventory Monitoring and Modeling System (GIMMS) NDVI dataset (GIMMS NDVI3g) was used as a proxy for vegetation growth during the 1982–2015 period (Pinzon and Tucker 2014). The long-term monthly gridded NDVI data offer the potential to monitor vegetation responses to climate change (Yuan *et al* 2019, Chen *et al* 2019a, Ma *et al* 2021, Su *et al* 2023). The monthly gridded PDSI data were obtained from the TerraClimate high-spatial-resolution climate dataset (Abatzoglou *et al* 2018). We used PDSI as a proxy for water availability to estimate relative dryness. For example, a PDSI value > 4 represents very wet conditions, while a PDSI < -4 represents an extreme drought.

The land use and land change data were obtained from the HIstoric Land Dynamics Assessment+ (HILDA+) project to determine those vegetated regions in the Northern Hemisphere mid-latitudes for each growing season (Winkler *et al* 2021). To focus on our goals, we ignored the interannual transformation between vegetated and non-vegetated areas. That is, we used the intersection of all the vegetation layers to ensure that each grid cell was a vegetated region from the beginning to the end of our study period. The aridity index (AI) was used to identify arid, semi-arid, sub-humid, and humid zones (Zomer *et al* 2022).

The monthly gridded climate data, including air temperature (Tmp), precipitation (Pre), VPD, downward surface shortwave radiation (Srad), and soil moisture (SM), were also obtained from the TerraClimate dataset (Abatzoglou *et al* 2018). The monthly gridded atmospheric CO_2 data were obtained from the Copernicus atmosphere monitoring service (CAMS) reanalysis dataset. The monthly gridded evapotranspiration (ET) data were obtained from the breathing earth system simulator (BESS) model outputs (Li *et al* 2023a).

All the gridded data were aggregated to a $0.1^\circ \times 0.1^\circ$ spatial resolution using the nearest neighbor resampling method. We defined the active growing season as April–October in each year, and then calculated the seven-month mean NDVI value for each year from 1982 to 2015 as an annual indicator of vegetation growth. The data we used in this study are publicly available (more details can be found in the 'Data availability statements' section).

2.2. Methods

The Theil–Sen estimator (Theil 1950, Sen 1968) with the non-parametric Mann–Kendall test (Mann 1945, Kendall 1948) was used to estimate the linear trends in NDVI, PDSI, and their correlation coefficients for each grid cell. This trend estimation method is insensitive to outliers and is thus more accurate and robust for long-term satellite observations. The formula for the Theil-Sen estimator is as follows:

$$\varphi = Median\frac{(x_j - x_i)}{(j-i)}\ (\forall j > i) \tag{1}$$

where φ is the trend of the factor x in the time series, x_j and x_i represent the observed values of the factor x corresponding to moments j and i, respectively, and *Median* is the median function. The formulas for the non-parametric Mann–Kendall test are as follows:

$$Z = \begin{cases} \frac{S-1}{\sqrt{var(S)}} & (S > 0) \\ 0 \quad \text{if} & (S = 0) \\ \frac{S+1}{\sqrt{var(S)}} & (S < 0) \end{cases} \tag{2}$$

$$S = \sum_{i=1}^{n-1}\sum_{j=i+1}^{n} sgn\left(x_j - x_i\right) \tag{3}$$

$$sgn\left(x_j - x_i\right) = \begin{cases} 1\ \left(x_j - x_i > 0\right) \\ 0 \text{ if } \left(x_j - x_i = 0\right) \\ -1\ \left(x_j - x_i < 0\right) \end{cases} \tag{4}$$

where Z represents the significance statistic of the factor x, S is the statistic of the factor x, $var(S)$ is the sample variance of the approximate standard normal distribution of S, x_j and x_i represent the observed values of the factor x corresponding to moments j and i, respectively, n denotes the length of the time series, and *sgn* is the positive and negative sign function. In this study, the significant level of confidence is 0.05 ($p < 0.05$), corresponding to $|Z| > 1.96$.

The Spearman's rank NDVI-PDSI correlation coefficient was used to characterize the Rvw for each grid cell (Jiao *et al* 2021). A significant positive NDVI-PDSI correlation coefficient implies that NDVI increases with wetting and decreases with drying, suggesting that vegetation growth in the region is constrained by water deficit. In contrast, a significant negative NDVI-PDSI correlation coefficient implies that NDVI decreases with wetting and increases with drying, suggesting that vegetation growth is constrained by water surplus. The grid cells with non-significant NDVI-PDSI correlation coefficients indicate that vegetation growth is not clearly constrained by water availability. We used the two-tailed t-test to determine whether the NDVI-PDSI correlation coefficient was significant at 0.05 confidence level ($p < 0.05$). We also used 25 10 year moving windows spanning from 1982 to 2015 (i.e. 1982–1991, 1983–1992, …, 2006–2015) to estimate the trend in the NDVI-PDSI correlation coefficient for each grid cell.

The random forest regression algorithm was applied to simulate the NDVI-PDSI correlation coefficient for each grid cell using Tmp, Pre, VPD, Srad, SM, and atmospheric CO_2. The random forest regression models were trained pixel by pixel using the function 'TreeBagger' in MATLAB R2023a software (The MathWorks, Inc., Natick, MA, USA). The 'numTrees' parameter was set to '200' to meet our requirements for accuracy and robustness. The dominant driver (i.e. one of those forcing factors) was identified by ranking the feature importance. To examine the effect of linear trends on the models, we used the trend estimation method described above to detrend the time-series data, and then retrained the random forest regression models based on the detrended data. To further reveal how the dominant driver affected changes in the Rvw, we conducted the partial correlation analysis to evaluate its roles on NDVI and PDSI individually (Yuan *et al* 2019, Song *et al* 2022). The effects of other drivers on the correlation between the dominant driver and NDVI/PDSI were excluded. In addition, we introduced WUE to explore the indirect effect of the dominant driver on water availability. We calculated WUE_{NDVI} with ET data as follows (Tian *et al* 2021):

$$WUE_{NDVI} = NDVI\ /\ ET \tag{5}$$

where WUE_{NDVI} is defined as the ratio of NDVI to ET. The code files and corresponding outputs for our core findings are publicly available in the Figshare data repository (https:https://doi.org/10.6084/m9.figshare.25140008.v3).

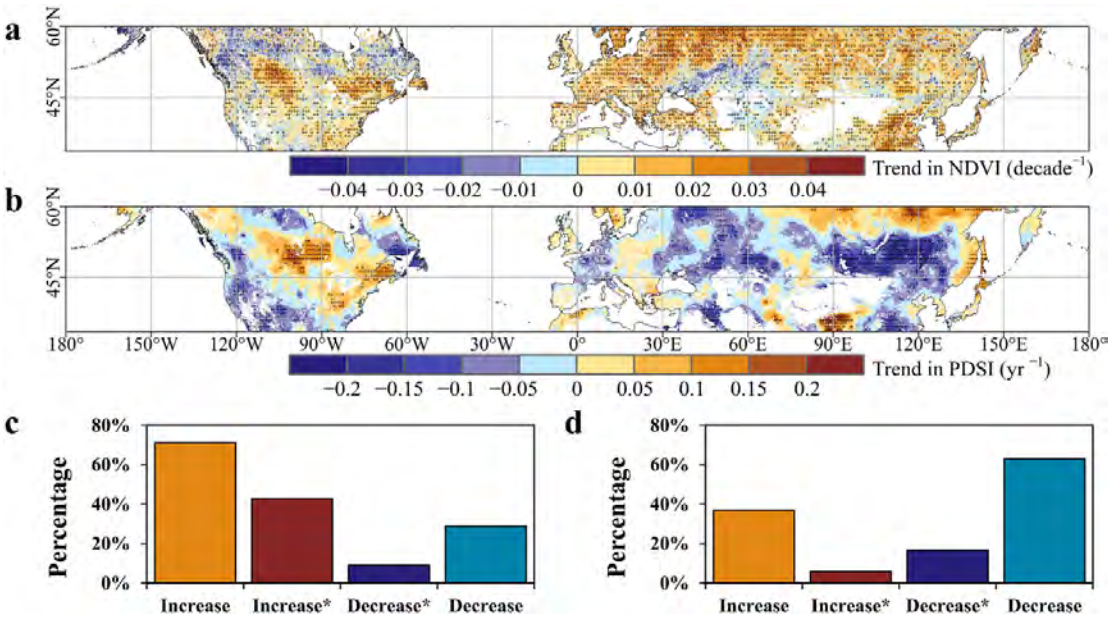

Figure 1. Spatial patterns of the trends in vegetation growth and water availability in the Northern Hemisphere mid-latitudes from 1982 to 2015. (a) Spatial distribution of the trends in normalized difference vegetation index (NDVI). (b) Spatial distribution of the trends in Palmer drought severity index (PDSI). The black crosses in (a), (b) indicate a significant trend (Mann–Kendall test: $p < 0.05$). (c), (d) are the statistical distributions of (a), (b), respectively.

3. Results

3.1. Recent trends in vegetation growth and water availability under climate change

We used the Theil-Sen estimator combined with the non-parametric Mann–Kendall test to estimate changes in vegetation growth and water availability for each grid cell in the Northern Hemisphere mid-latitudes during 34 active growing seasons (i.e. from April to October) from 1982 to 2015. Global vegetation growth was considered to be widespread increasing and was known as 'greening' (Myneni *et al* 1997, Zhu *et al* 2016, Chen *et al* 2019b). In this study, our results showed that NDVI has increased in most areas (figure 1(a)). Specifically, 71.08% of grid cells exhibited an increase in NDVI during the period (42.88% with a significant increase, Mann–Kendall test: $p < 0.05$), while only 9.02% of grid cells had a significant decrease (Mann–Kendall test: $p < 0.05$) (figure 1(c)). However, we found that the area with a significant trend in PDSI was much smaller than that with a significant trend in NDVI (figure 1(b)). Specifically, 16.56% of grid cells exhibited a significant decrease in PDSI during the period (Mann–Kendall test: $p < 0.05$), while only 5.74% of grid cells had a significant increase (Mann–Kendall test: $p < 0.05$) (figure 1(d)). Overall, we found the trends in NDVI and PDSI were asynchronous, suggesting a weak coupling between them.

3.2. Spatiotemporal patterns of the Rvw in the Northern Hemisphere mid-latitudes

We evaluated spatiotemporal patterns of the Rvw in the Northern Hemisphere mid-latitudes over the past three decades. Our results showed a strong NDVI-PDSI correlation for most grid cells, suggesting strong water constraints on vegetation growth (figure 2(a)). Specifically, 55.80% of grid cells had a positive NDVI-PDSI correlation (23.02% with a significant correlation, two-tailed t-test: $p < 0.05$), and 8.93% of grid cells had a significant negative NDVI-PDSI correlation (two-tailed t-test: $p < 0.05$) (figure 2(c)). We found that vegetation growth was constrained primarily by water deficit and secondarily by water surplus. In addition, the differences in NDVI-PDSI correlations were more pronounced across different climatic zones. The NDVI-PDSI correlations were 0.38 ± 0.25, 0.28 ± 0.28, -0.01 ± 0.25, and -0.11 ± 0.23 in arid ($AI < 0.2$), semi-arid ($0.2 < AI < 0.5$), sub-humid ($0.5 < AI < 0.65$), and humid ($AI > 0.65$) zones, respectively. Moreover, we analyzed the trend in the NDVI-PDSI correlation coefficient for each grid cell across the 25 10 year moving windows during the 1982–2015 period (figure 2(b)). The results indicated that the NDVI-PDSI correlation coefficients in 54.60% of grid cells had an increasing trend (28.72% with a significant correlation, Mann–Kendall test: $p < 0.05$), while 21.95% of grid cells had a significant decreasing trend (Mann–Kendall test: $p < 0.05$) (figure 2(d)).

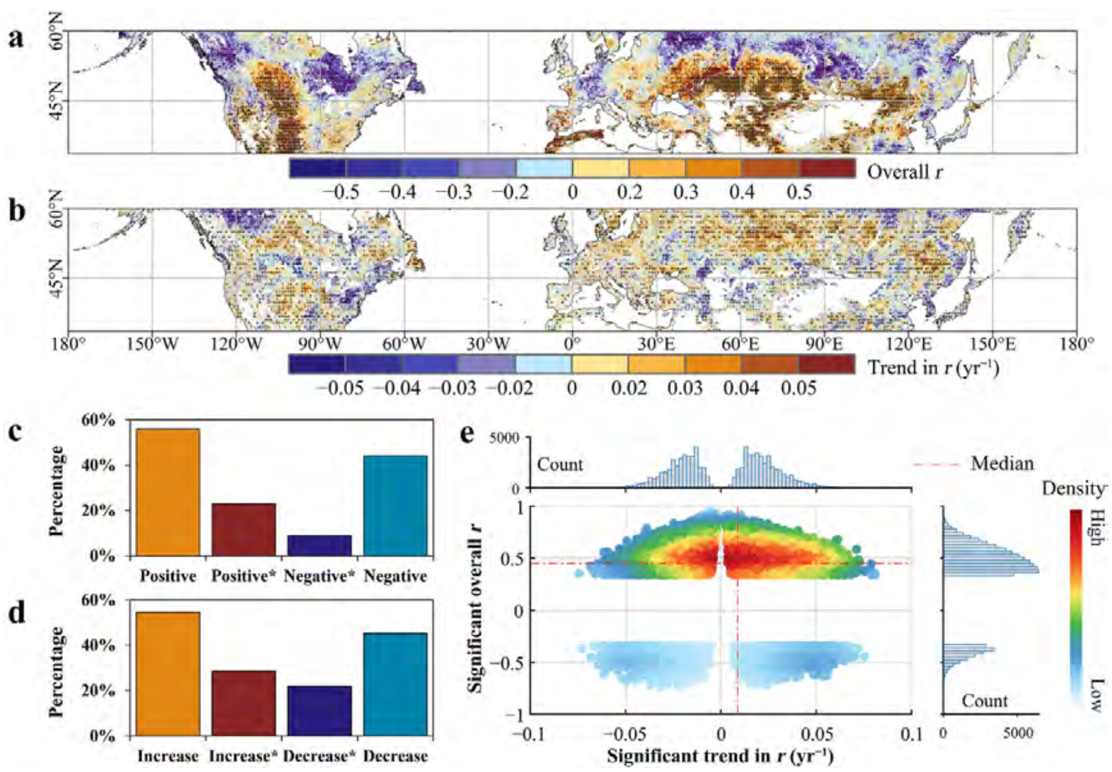

Figure 2. Spatiotemporal patterns of the relationship between vegetation growth and water availability in the Northern Hemisphere mid-latitudes from 1982 to 2015. (a) Spatial distribution of the correlation coefficients (r) between normalized difference vegetation index (NDVI) and Palmer drought severity index (PDSI) for the entire study period. (b) Spatial distribution of the trends in r between NDVI and PDSI across the 25 10 year moving windows. The black crosses in (a), (b) indicate a significant correlation (two-tailed t-test: $p < 0.05$) and a significant trend (Mann-Kendall test: $p < 0.05$), respectively. (c), (d) are the statistical distributions of (a), (b), respectively; (e) Scatter plots of the significant r versus the significant trend in r.

Furthermore, we mapped the scatter plots of the significant NDVI-PDSI correlation coefficient versus the corresponding significant trend, and found that more grid cells were in the first quadrant (upper right) (figure 2(e)). The NDVI-PDSI correlation was significantly positive in more areas (the median = 0.45, two-tailed t-test: $p < 0.05$), and at the same time the corresponding trend was also significantly increasing (the median = 0.01 yr^{-1}, Mann-Kendall test: $p < 0.05$). There were also some grid cells in the third quadrant (lower left) that exhibited a significant negative NDVI-PDSI correlation, while the corresponding trend was significantly decreasing. Recent water constraints (including water deficit and water surplus) on vegetation growth were increasing in nearly half of the region. Overall, we revealed that the Rvw has become closer in the Northern Hemisphere mid-latitudes over the past three decades.

3.3. Different spatiotemporal patterns of the Rvw across croplands, grasslands, and forests

We further investigated spatiotemporal patterns of the Rvw across three ecosystems: croplands, grasslands, and forests in the Northern Hemisphere mid-latitudes over the past three decades. Our results showed the differences in the NDVI-PDSI correlation for croplands, grasslands, and forests during the entire study period (figure 3(a)). The median of the significant NDVI-PDSI correlation coefficients for croplands (0.46, two-tailed t-test: $p < 0.05$) was weaker than that for grasslands (0.50, two-tailed t-test: $p < 0.05$) (figure 3(c)). Compared to less managed or unmanaged grasslands, irrigation and management practices seem to be effective against water constraints on cultivated vegetation (Jägermeyr *et al* 2016). However, we found that the significant NDVI-PDSI correlation coefficients for forests were negative in more areas (the median = −0.39, two-tailed t-test: $p < 0.05$) (figure 3(c)). Tree growth in these areas was barely limited by water deficit; conversely, they were constrained by water surplus due to excess precipitation-related energy shortages (Myneni *et al* 1997, Jiao *et al* 2021). The forest regions were relatively wetter and cooler, and these trees with deep root systems also appear to resist water deficit on their growth very well (Teskey *et al* 2014, Brunner *et al* 2015, Castagneri *et al* 2021). Moreover, we analyzed the differences in the trend of the NDVI-PDSI correlation coefficients among croplands, grasslands, and forests across the 25 10 year moving windows (figure 3(b)). The results showed that the median of the trend in the NDVI-PDSI correlation for croplands was surprisingly consistent with that for forests (approximately 0.0136 yr^{-1}, Mann-Kendall

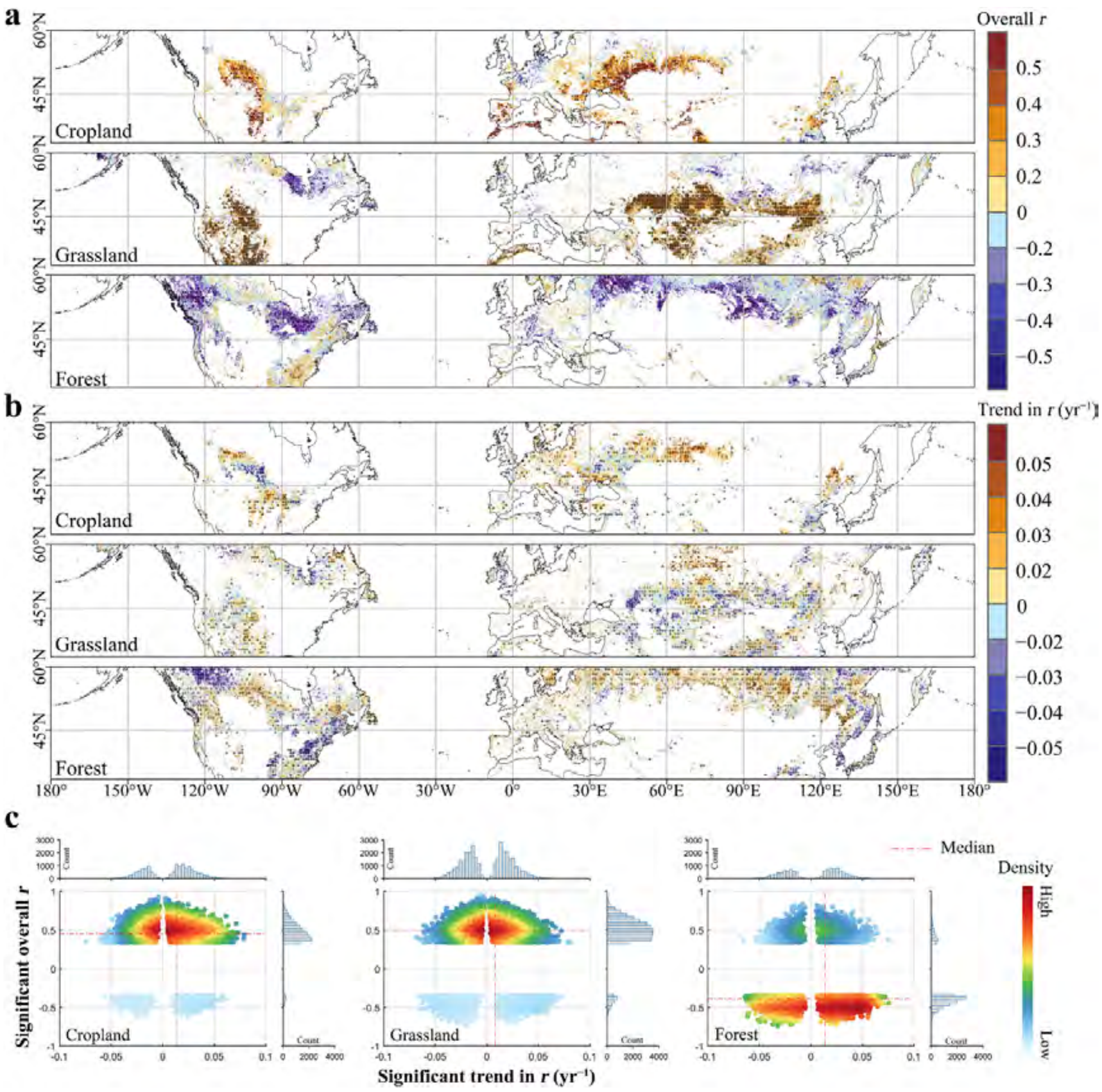

Figure 3. Spatiotemporal patterns of the relationship between vegetation growth and water availability for croplands, grasslands, and forests in the Northern Hemisphere mid-latitudes from 1982 to 2015. (a) Spatial distribution of the correlation coefficients (r) between normalized difference vegetation index (NDVI) and Palmer drought severity index (PDSI) for croplands, grasslands, and forests during the entire study period. (b) Spatial distribution of the trends in r between NDVI and PDSI for croplands, grasslands, and forests across the 25 10 year moving windows. The black crosses in (a), (b) indicate a significant correlation (two-tailed t-test: $p < 0.05$) and a significant trend (Mann–Kendall test: $p < 0.05$), respectively. (c) Scatter plots of the significant r versus the significant trend in r for croplands, grasslands, and forests.

test: $p < 0.05$), being about 1.7 times higher than that for grasslands (0.0078 yr^{-1}, Mann-Kendall test: $p < 0.05$) (figure 3(c)). Overall, we found that croplands and grasslands were primarily and becoming increasingly constrained more by water deficit, while forests were primarily but becoming decreasingly constrained by water surplus.

3.4. Dominant drivers of changes in the Rvw over the past three decades

To evaluate the dominant driver of changes in the Rvw, we applied the random forest regression algorithm to simulate the NDVI-PDSI correlation coefficients using climate and atmospheric CO_2 data in the Northern Hemisphere mid-latitudes from 1982 to 2015. We trained the random forest regression models pixel by pixel and then identified the dominant driver for each grid cell by ranking the feature importance (figure 4(a)). Our results showed that Tmp, Pre, VPD, Rad, SM, and atmospheric CO_2 dominated the NDVI-PDSI correlation coefficients in 10.44%, 10.62%, 11.50%, 11.37%, 10.74%, and 45.32% of grid cells, respectively. This finding was essentially consistent across the three ecosystems: croplands, grasslands, and forests (figure 4(c)). Surprisingly, atmospheric CO_2 played a dominant role in influencing the trend of the Rvw for nearly half of grid cells. To examine whether the dominant driver of changes in the Rvw were influenced by long-term trends in the inputs, we repeated the same analysis based on the linear detrended time series. The detrended results of both spatial patterns (figure 4(b))

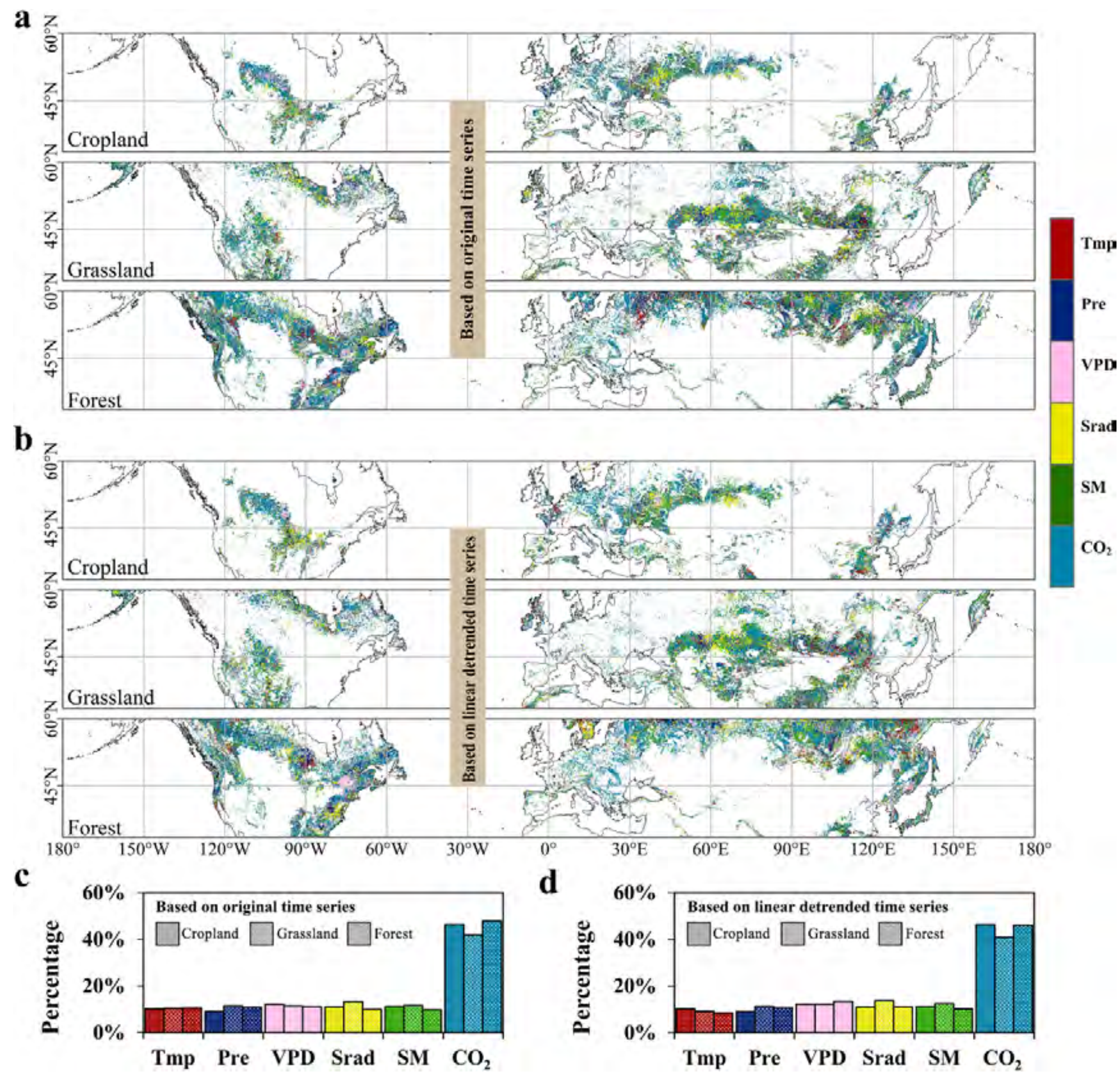

Figure 4. Spatial distribution of the dominant driver of the relationship between vegetation growth and water availability for croplands, grasslands, and forests in the Northern Hemisphere mid-latitudes from 1982 to 2015. (a) Spatial distribution of the dominant driver influencing the correlation coefficients (r) between normalized difference vegetation index (NDVI) and Palmer drought severity index (PDSI) for croplands, grasslands, and forests. (b) Spatial distribution of the dominant driver influencing r for croplands, grasslands, and forests based on the linear detrended time series. The drivers include air temperature (Tmp), precipitation (Pre), vapor pressure deficit (VPD), downward surface shortwave radiation (Srad), soil moisture (SM), and atmospheric carbon dioxide (CO_2). (c), (d) are the statistical distributions of (a, b), respectively.

and area statistics (figure 4(d)) showed agreement with our above findings. Overall, we found that atmospheric CO_2 has tightened the Rvw across croplands, grasslands, and forests in the Northern Hemisphere mid-latitudes over the past three decades.

4. Discussion

Previous studies have reported that the increases in vegetative growth were mainly due to the CO_2 fertilization effect, climate change, and human activities (Myneni *et al* 1997, Piao *et al* 2015, 2020, Lu *et al* 2016, Zhu *et al* 2016, Chen *et al* 2019b). In this study, we explored the long-term trends in NDVI and PDSI to determine whether there was a strong coupling between them. Our results showed that changes in NDVI and PDSI were asynchronous in the Northern Hemisphere mid-latitudes over the past three decades. Compared to the observed significant long-term trends in NDVI, PDSI as a proxy for water availability may exhibit cyclical short-term or non-significant long-term trends (Feng and Fu 2013, Huang *et al* 2016, Berg and McColl 2021). The mismatched trends between vegetation growth and water availability can minimize the effect of co-linearity on the NDVI-PDSI correlation, which is beneficial for our following analyses.

One of our main goals is to evaluate spatiotemporal patterns of the Rvw in the Northern Hemisphere mid-latitudes over the past three decades. The results indicated that the Rvw was getting closer in more areas over the period, but there were differences across ecosystems. The Rvw was getting stronger in most croplands and grasslands;

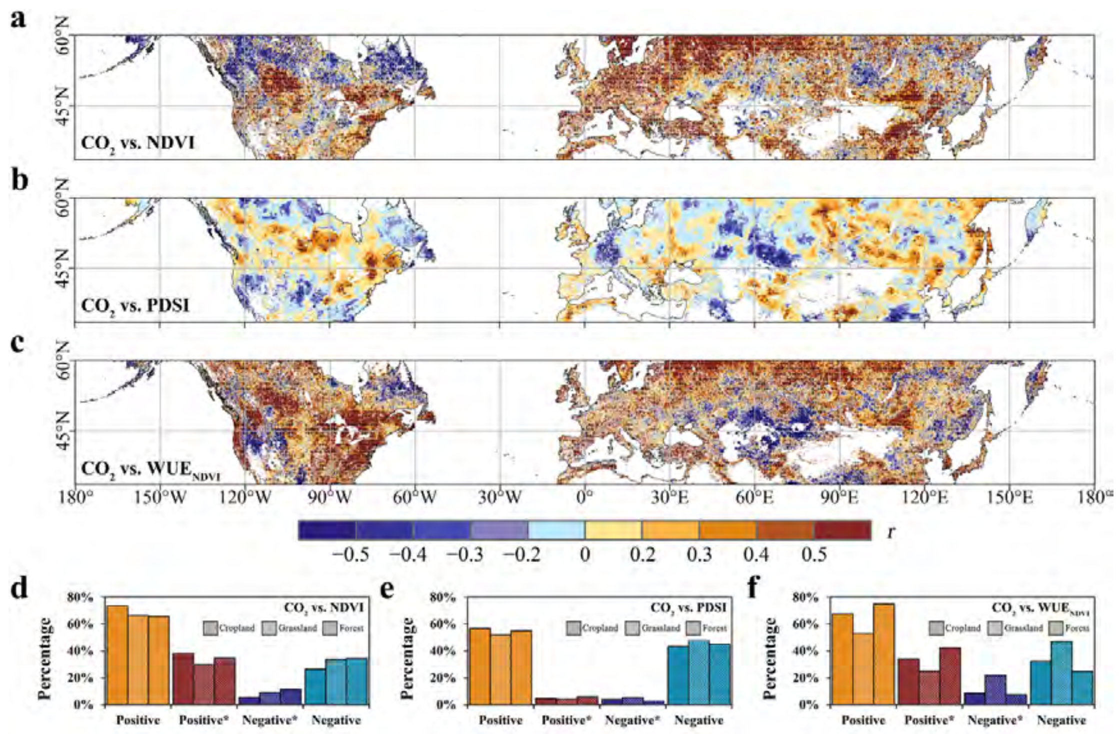

Figure 5. Partial correlation analyses of atmospheric carbon dioxide (CO_2) with normalized difference vegetation index (NDVI), Palmer drought severity index (PDSI), and NDVI's water use efficiency (WUE_{NDVI}) in the Northern Hemisphere mid-latitudes from 1982 to 2015. (a) Spatial distribution of the partial correlation coefficients (partial r) between atmospheric CO_2 and NDVI. (b) Spatial distribution of the partial r between atmospheric CO_2 and PDSI. (c) Spatial distribution of the partial r between atmospheric CO_2 and WUE_{NDVI}. The black crosses indicate a significant partial correlation (two-tailed t-test: $p < 0.05$). We conducted partial correlation analyses of atmospheric CO_2 with NDVI, PDSI, and WUE_{NDVI} by excluding the effects of air temperature (Tmp), precipitation (Pre), vapor pressure deficit (VPD), downward surface shortwave radiation (Srad), and soil moisture (SM). (d)–(e) are the statistical distributions of (a)–(c) for croplands, grasslands, and forests, respectively.

however, it was getting weaker in most forests. These findings were in line with previous studies (Madani *et al* 2020, Jiao *et al* 2021, Denissen *et al* 2022, Liu *et al* 2023). We also found that croplands and grasslands were primarily and becoming increasingly constrained more by water deficit, while forests were primarily but becoming decreasingly constrained by water surplus. Whether forests would shift to be limited by water deficit remains unknown, but it could be projected that croplands and grasslands might face more drought risk in the future (Ciais *et al* 2005, Pokhrel *et al* 2021, Denissen *et al* 2022). This poses a serious threat to agricultural and livestock production in the Northern Hemisphere mid-latitudes (Sinclair and Rufty 2012, Lesk *et al* 2016, Hendrawan *et al* 2022).

The core finding of this study is to reveal the dominant driver of changes in the Rvw in the Northern Hemisphere mid-latitudes over the past three decades. We employed random forest regression models to conduct the attribution analysis (Yuan *et al* 2019, Chang *et al* 2023, Dong *et al* 2023, Yang *et al* 2024). In this study, we found that the dominant driver of changes in the NDVI-PDSI correlation was atmospheric CO_2 in more than 45% of grid cells. Since the Industrial Revolution, atmospheric CO_2 as a clearly observed factor were widely involved in the exchange of water, carbon, and energy between the land surface and the atmosphere (Sellers *et al* 1997, Novick *et al* 2016). However, how atmospheric CO_2 affected NDVI and PDSI, and thus changes in the Rvw, was not clear. Therefore, we conducted the partial correlation analysis to evaluate its roles on NDVI and PDSI individually (Yuan *et al* 2019, Song *et al* 2022).

Considering that atmospheric CO_2 was the dominant driver of changes in the Rvw for both croplands, grasslands, and forests, we mapped the partial correlation results without distinguishing the ecosystems (figures 5(a)–(c)). Our results showed that 73.65%, 66.35%, and 65.71% of grid cells had a positive partial correlation between atmospheric CO_2 and NDVI for croplands, grasslands, and forests, respectively (37.87%, 29.47%, and 34.66% with a significant correlation, two-tailed t-test: $p < 0.05$) (figure 5(d)). The fertilization effect due to elevated CO_2 concentrations can boost vegetation growth and greenness (Schimel *et al* 2014, Wang *et al* 2020). However, the partial correlation between atmospheric CO_2 and PDSI was barely significant for the three ecosystems (only 3.89%, 5.41%, and 2.43% with a significant negative correlation, two-tailed t-test: $p < 0.05$) (figure 5(e)). The results showed that elevated CO_2 concentrations did not directly enhance water availability while boosting vegetation growth. Notably, we found that 67.65%, 52.88%, and 75.09% of grid cells had a positive partial correlation between atmospheric CO_2 and WUE_{NDVI} for croplands, grasslands, and forests, respectively (34.16%, 25.25%, and 42.43% with a significant correlation, two-tailed t-test: $p < 0.05$) (figure 5(f)). It seems that elevated CO_2 concentrations played a role in improving WUE_{NDVI}, thereby indirectly reducing vegetation water demand (equivalent to enhancing water availability). Our findings were supported by previous studies (Keenan *et al* 2013, Lu *et al* 2016, Li *et al* 2021, 2023b).

5. Conclusion

In this study, we conducted a comprehensive evaluation of changes in the Rvw in the Northern Hemisphere mid-latitudes over the past three decades. Our findings revealed a closer Rvw hidden within their asynchronous trends. The NDVI-PDSI correlation was significantly positive in more areas than those with a significantly negative correlation, showing vegetation growth was constrained primarily by water deficit and secondarily by water surplus in this region during the period. Besides, we used 25 10 year moving windows spanning from 1982 to 2015 to estimate the trend in the NDVI-PDSI correlation coefficient for each grid cell. The results indicated that vegetation growth has become increasingly constrained by water deficit in most areas but also by water surplus in a few areas. For different ecosystems, croplands and grasslands were primarily and increasingly constrained by water deficit; however, forests were primarily but decreasingly constrained by water surplus. Croplands and grasslands would face more drought risk in the future, posing a serious threat to livestock and agricultural production. Considering the potential for forests to be more constrained by water deficit, their future drought risk should not be underestimated. Further analyses indicated that atmospheric CO_2 as the dominant driver explained changes in the Rvw in most areas. This finding was essentially consistent across croplands, grasslands, and forests. We also found that the CO_2 fertilization effect can enhance NDVI; however, there was no significant correlation between atmospheric CO_2 and PDSI. To clarify the role of elevated CO_2 concentrations in boosting vegetation growth while regulating water availability, we introduced WUE_{NDVI} for an additional analysis. The results showed that atmospheric CO_2 and WUE_{NDVI} were highly correlated, suggesting that elevated CO_2 concentrations could indirectly enhance water availability by improving WUE_{NDVI}. In summary, our findings highlight that elevated CO_2 concentrations contribute to a closer Rvw by jointly enhancing both of them. Therefore, further understanding of climate change impacts on vegetation dynamics remains urgently needed for a full assessment of drought risk in the current and future.

Data availability statement

The GIMMS NDVI3g dataset is available at https://10.7289/V5ZG6QH9. The monthly gridded PDSI and climate data are available at www.climatologylab.org/terraclimate.html. The HILDA+ land use change data are available at https://10.1594/PANGAEA.921846. The AI dataset is available at https://10.6084/m9.figshare.7504448.v6. The monthly gridded atmospheric CO_2 data are available at https://ads.atmosphere.copernicus.eu/cdsapp#!/dataset/cams-global-greenhouse-gas-inversion?tab=overview. The monthly gridded ET data are available at https://www.environment.snu.ac.kr/bessv2. The code files and corresponding outputs are available at https://doi.org/10.6084/m9.figshare.25140008.v3.

All data that support the findings of this study are included within the article (and any supplementary files).

Acknowledgments

This research was supported by the National Natural Science Foundation of China (32301395), the Nanfan Special Project of the Chinese Academy of Agricultural Sciences (YBXM2305), and the Open Competition Project of Heilongjiang Province of China (2021ZXJ05A03). We would like to thank all the producers of the datasets used in this study.

Conflict of interest

The authors have no competing interests to declare.

ORCID iDs

Yang Song https://orcid.org/0000-0002-4233-2682
Yahui Guo https://orcid.org/0000-0002-0099-0759
Shijie Li https://orcid.org/0000-0002-2419-9988
Wangyipu Li https://orcid.org/0000-0003-1960-3517
Xiuliang Jin https://orcid.org/0000-0002-6769-214X

References

Abatzoglou J T, Dobrowski S Z, Parks S A and Hegewisch K C 2018 TerraClimate, a high-resolution global dataset of monthly climate and climatic water balance from 1958–2015 *Sci. Data* **5** 170191

Abel C, Abdi A M, Tagesson T, Horion S and Fensholt R 2023 Contrasting ecosystem vegetation response in global drylands under drying and wetting conditions *Glob. Change Biol.* **29** 3954–69

Bastos A *et al* 2019 Contrasting effects of CO_2 fertilization, land-use change and warming on seasonal amplitude of Northern Hemisphere CO_2 exchange *Atmos. Chem. Phys.* **19** 12361–75

Berg A and McColl K A 2021 No projected global drylands expansion under greenhouse warming *Nat. Clim. Change* **11** 331–U71
Brunner I, Herzog C, Dawes M A, Arend M and Sperisen C 2015 How tree roots respond to drought *Front. Plant Sci.* **6** 547
Castagneri D, Vacchiano G, Hacket-Pain A, DeRose R J, Klein T and Bottero A 2021 Meta-analysis reveals different competition effects on tree growth resistance and resilience to drought *Ecosystems* **25** 30–43
Chang Q *et al* 2023 Soil moisture drives the spatiotemporal patterns of asymmetry in vegetation productivity responses across China *Sci. Total Environ.* **855** 158819
Chen C, He B, Yuan W, Guo L and Zhang Y 2019a Increasing interannual variability of global vegetation greenness *Environ. Res. Lett.* **14** 124005
Chen C *et al* 2019b China and India lead in greening of the world through land-use management *Nat. Sustain.* **2** 122–9
Chen Z, Wang W, Cescatti A and Forzieri G 2022 Climate-driven vegetation greening further reduces water availability in drylands *Glob. Change Biol.* **29** 1628–47
Ciais P *et al* 2005 Europe-wide reduction in primary productivity caused by the heat and drought in 2003 *Nature* **437** 529–33
Denissen J M C, Teuling A J, Pitman A J, Koirala S, Migliavacca M, Li W T, Reichstein M, Winkler A J, Zhan C and Orth R 2022 Widespread shift from ecosystem energy to water limitation with climate change *Nat. Clim. Change* **12** 677
Dong G Y *et al* 2023 Asymmetric response of primary productivity to precipitation anomalies in Southwest China *Agric. For. Meteorol.* **331** 109350
Doughty C E *et al* 2015 Drought impact on forest carbon dynamics and fluxes in Amazonia *Nature* **519** 78–U140
Feng S and Fu Q 2013 Expansion of global drylands under a warming climate *Atmos. Chem. Phys.* **13** 10081–94
Hendrawan V S A, Kim W, Touge Y, Ke S and Komori D 2022 A global-scale relationship between crop yield anomaly and multiscalar drought index based on multiple precipitation data *Environ. Res. Lett.* **17** 014037
Hsu H and Dirmeyer P A 2023 Soil moisture-evaporation coupling shifts into new gears under increasing CO_2 *Nat. Commun.* **14** 1162
Huang J, Yu H, Guan X, Wang G and Guo R 2016 Accelerated dryland expansion under climate change *Nat. Clim. Change* **6** 166
Huang K *et al* 2018 Enhanced peak growth of global vegetation and its key mechanisms *Nat. Ecol. Evol.* **2** 1897–905
Humphrey V, Zscheischler J, Ciais P, Gudmundsson L, Sitch S and Seneviratne S I 2018 Sensitivity of atmospheric CO_2 growth rate to observed changes in terrestrial water storage *Nature* **560** 628
Jägermeyr J, Gerten D, Schaphoff S, Heinke J, Lucht W and Rockström J 2016 Integrated crop water management might sustainably halve the global food gap *Environ. Res. Lett.* **11** 025002
Jiao W, Wang L, Smith W K, Chang Q, Wang H and D'Odorico P 2021 Observed increasing water constraint on vegetation growth over the last three decades *Nat. Commun.* **12** 3777
Jung M *et al* 2010 Recent decline in the global land evapotranspiration trend due to limited moisture supply *Nature* **467** 951–4
Keenan T F, Hollinger D Y, Bohrer G, Dragoni D, Munger J W, Schmid H P and Richardson A D 2013 Increase in forest water-use efficiency as atmospheric carbon dioxide concentrations rise *Nature* **499** 324–7
Kendall M G 1948 *Rank Correlation Methods* (C. Griffin)
Lesk C, Rowhani P and Ramankutty N 2016 Influence of extreme weather disasters on global crop production *Nature* **529** 84
Li B, Ryu Y, Jiang C, Dechant B, Liu J, Yan Y and Li X 2023a BESSv2.0: a satellite-based and coupled-process model for quantifying long-term global land–atmosphere fluxes *Remote Sens. Environ.* **295** 113696
Li F, Guo D, Gao X and Zhao X 2021 Water deficit modulates the CO_2 fertilization effect on plant gas exchange and leaf-level water use efficiency: a meta-analysis *Front. Plant Sci.* **12** 775477
Li F, Xiao J, Chen J, Ballantyne A, Jin K, Li B, Abraha M and John R 2023b Global water use efficiency saturation due to increased vapor pressure deficit *Science* **381** 672–7
Liu K, Li X, Wang S and Zhou G 2023 Past and future adverse response of terrestrial water storages to increased vegetation growth in drylands *npj Clim. Atmos. Sci.* **6** 113
Lu X, Wang L and McCabe M F 2016 Elevated CO_2 as a driver of global dryland greening *Sci. Rep.* **6** 20716
Ma C, Li T and Liu P 2021 GIMMS NDVI3g+ (1982–2015) response to climate change and engineering activities along the Qinghai–Tibet railway *Ecol. Indic.* **128** 107821
Madani N, Parazoo N C, Kimball J S, Ballantyne A P, Reichle R H, Maneta M, Saatchi S, Palmer P I, Liu Z and Tagesson T 2020 Recent amplified global gross primary productivity due to temperature increase is offset by reduced productivity due to water constraints *AGU Adv.* **1** e2020AV000180
Mann H B 1945 Nonparametric tests against trend *Econometrica* **13** 245–59
Myneni R B, Keeling C D, Tucker C J, Asrar G and Nemani R R 1997 Increased plant growth in the northern high latitudes from 1981 to 1991 *Nature* **386** 698–702
Nemani R R, Keeling C D, Hashimoto H, Jolly W M, Piper S C, Tucker C J, Myneni R B and Running S W 2003 Climate-driven increases in global terrestrial net primary production from 1982 to 1999 *Science* **300** 1560–3
Novick K A *et al* 2016 The increasing importance of atmospheric demand for ecosystem water and carbon fluxes *Nat. Clim. Change* **6** 1023–7
Peng J, Wu C, Zhang X, Wang X and Gonsamo A 2019 Satellite detection of cumulative and lagged effects of drought on autumn leaf senescence over the Northern Hemisphere *Glob. Change Biol.* **25** 2174–88
Peters W *et al* 2018 Increased water-use efficiency and reduced CO_2 uptake by plants during droughts at a continental scale *Nat. Geosci.* **11** 744
Piao S *et al* 2020 Characteristics, drivers and feedbacks of global greening *Nat. Rev. Earth Environ.* **1** 14–27
Piao S *et al* 2015 Detection and attribution of vegetation greening trend in China over the last 30 years *Glob. Change Biol.* **21** 1601–9
Pinzon J E and Tucker C J 2014 A non-stationary 1981–2012 AVHRR NDVI3g time series *Remote Sens.* **6** 6929–60
Pokhrel Y *et al* 2021 Global terrestrial water storage and drought severity under climate change *Nat. Clim. Change* **11** 226–33
Schimel D, Stephens B B and Fisher J B 2014 Effect of increasing CO_2 on the terrestrial carbon cycle *Proc. Natl Acad. Sci.* **112** 436–41
Schwalm C R *et al* 2017 Global patterns of drought recovery *Nature* **548** 202
Sellers P J *et al* 1997 Modeling the exchanges of energy, water, and carbon between continents and the atmosphere *Science* **275** 502–9
Sen P K 1968 Estimates of the regression coefficient based on Kendall's Tau *J. Am. Stat. Assoc.* **63** 1379–89
Shi S, Yu J, Wang F, Wang P, Zhang Y and Jin K 2021 Quantitative contributions of climate change and human activities to vegetation changes over multiple time scales on the Loess Plateau *Sci. Total Environ.* **755** 142419
Sinclair T R and Rufty T W 2012 Nitrogen and water resources commonly limit crop yield increases, not necessarily plant genetics *Global Food Security-Agriculture Policy Economics and Environment* **1** 94–98
Smith T and Boers N 2023 Global vegetation resilience linked to water availability and variability *Nat. Commun.* **14** 498
Song Y, Jiao W, Wang J and Wang L 2022 Increased global vegetation productivity despite rising atmospheric dryness over the last two decades *Earths Future* **10** e2021EF002634
Su Y, Chen S, Li X, Ma S, Xie T, Wang J, Yan D, Chen J, Feng M and Chen F 2023 Changes in vegetation greenness and its response to precipitation seasonality in Central Asia from 1982 to 2022 *Environ. Res. Lett.* **18**

Teskey R, Wertin T, Bauweraerts I, Ameye M, McGuire M A and Steppe K 2014 Responses of tree species to heat waves and extreme heat events *Plant Cell Environ.* **38** 1699–712

Theil H 1950 A rank-invariant method of linear and polynomial regression analysis *Proc. R. Netherlands Acad. Sci.* **53** part I: 386–92; part II: 521–25; part III: 1397–412

Tian J, Zhang Z, Kong R, Zhu B, Zhang F, Jiang S and Chen X 2021 Changes in water use efficiency and their relations to climate change and human activities in three forestry regions of China *Theor. Appl. Climatol.* **144** 1297–310

Vicente-Serrano S M *et al* 2013 Response of vegetation to drought time-scales across global land biomes *Proc. Natl Acad. Sci. USA* **110** 52–57

Wang S *et al* 2020 Recent global decline of CO_2 fertilization effects on vegetation photosynthesis *Science* **370** 1295–300

Wei X, He W, Zhou Y, Cheng N, Xiao J, Bi W, Liu Y, Sun S and Ju W 2023 Increased sensitivity of global vegetation productivity to drought over the recent three decades *J. Geophys. Res.* **128** e2022JD037504

Winkler K, Fuchs R, Rounsevell M and Herold M 2021 Global land use changes are four times greater than previously estimated *Nat. Commun.* **12** 2501

Wu X *et al* 2017 Differentiating drought legacy effects on vegetation growth over the temperate Northern Hemisphere *Glob. Change Biol.* **24** 504–16

Yang Y, Yin J, Kang S, Slater L, Gu X and Volchak A 2024 Quantifying the drivers of terrestrial drought and water stress impacts on carbon uptake in China *Agric. For. Meteorol.* **344** 109817

Yuan W *et al* 2019 Increased atmospheric vapor pressure deficit reduces global vegetation growth *Sci. Adv.* **5** eaax1396

Zhao J, Feng H, Xu T, Xiao J, Guerrieri R, Liu S, Wu X, He X and He X 2021a Physiological and environmental control on ecosystem water use efficiency in response to drought across the northern hemisphere *Sci. Total Environ.* **758** 143599

Zhao W, Yu X, Jiao C, Xu C, Liu Y and Wu G 2021b Increased association between climate change and vegetation index variation promotes the coupling of dominant factors and vegetation growth *Sci. Total Environ.* **767** 144669

Zhu Z *et al* 2016 Greening of the Earth and its drivers *Nat. Clim. Change* **6** 791

Zomer R J, Xu J C and Trabucco A 2022 Version 3 of the global aridity index and potential evapotranspiration database *Sci. Data* **9** 409